



Short Communication

Zirconium(IV)-modified silica@magnetic nanocomposites: Fabrication, characterization and application as efficient, selective and reusable nanocatalysts for Friedel–Crafts, Knoevenagel and Pechmann condensation reactions



R.K. Sharma*, Yukti Monga, Aditi Puri

Department of Chemistry, University of Delhi, Delhi, India

ARTICLE INFO

Article history:

Received 21 January 2013

Received in revised form 15 February 2013

Accepted 15 February 2013

Available online 22 February 2013

Keywords:

Zirconium

Magnetically retrievable

Grafting

Silica

Nano-hybrid

ABSTRACT

A highly efficient and magnetically retrievable zirconium(IV) based nanocatalyst has been synthesized by covalent grafting of 3-hydroxy-2-methyl-1,4-naphthoquinone onto amine functionalized silica coated magnetic nanoparticles followed by complexation with $ZrOCl_2$. The structural and magnetic properties of obtained nanocatalyst are identified by TEM, SEM, XRD, EDS, VSM and FT-IR analyses. The potential of resultant organic–inorganic hybrid nanocatalyst was effectively evaluated for the range of organic transformations such as Friedel–Crafts, Knoevenagel and Pechmann condensation reactions. The magnetically recoverable nano-hybrid catalyst presented high TON and chemoselectivity with the ease of reusability for multiple cycles without any appreciable loss in its catalytic activity.

© 2013 Elsevier B.V. All rights reserved.

1. Introduction

With the commencement of the modern era, a shift in emphasis in green chemistry is apparent with the desire to develop more environmental friendly routes to a myriad of materials. This shift has become more evident with the growth of nanotechnology [1]. In this respect, the development of marvelous ‘superparamagnetic nanoparticles’ creates remarkable buzz in the field of green chemistry as their use provides easy magnetic recovery from the reaction product [2,3]. But unfortunately, magnetic nanoparticles are prone to aggregate, which tend to limit their applications. To avoid this, formation of passive coating of inert material on the surface of iron oxide nanoparticles is necessary. Among various inorganic supports for stabilization, silica is very promising because of its good thermal and mechanical stability, easy availability and inexpensiveness, and simple covalent modification with organometallic moieties [4,5].

The importance of zirconium as a homogeneous catalyst has already been cited in the number of biologically and pharmaceutically significant organic transformations [6,7]. However these homogeneous catalysts endow with the metal contamination of products which may be harmful for human health as well as for environment. To meet the criteria of renewable and environmentally conscious

catalytic development, recently, we have reported the importance of zirconium modified silica gel as a heterogeneous catalyst for the synthesis of various biologically important molecules [8]. Continuing our aim to explore novel heterogeneous catalysts [9–12], recently we have moved with the upbringing nanotechnology using magnetically recoverable catalytic systems [13], and this time we report the novel silica based superparamagnetic zirconium(IV) nanocatalyst (Zr(IV)-HMNQ@ASMPs) for the synthesis of various industrially significant compounds via Friedel–Crafts, Knoevenagel condensation and Pechmann condensation reactions. The biological, pharmaceutical, medicinal, and therapeutic properties of bis-indolyl methanes [14], α,β -unsaturated carbonyl compounds [15] and coumarin derivatives [16] have been well established in the literature. Though, there are many synthetic routes to obtain these derivatives, but no one such reagent is commercialized to date. Also, the developed methods have several drawbacks such as unsatisfactory yields, stringent reaction conditions, use of toxic organic reagents and prolonged reaction time. Therefore, improvement of catalytic route in terms of environmentally benign and economical approach is highly desirable.

2. Experimental

2.1. General remarks

X-ray diffraction (XRD) was performed using a Bruker (D8 Advance). Transmission electron microscopy (TEM) images were acquired

* Corresponding author at: Department of Chemistry, University of Delhi, Delhi-110007, India. Tel./fax: +91 11 27666250.

E-mail address: rksharmagreenchem@hotmail.com (R.K. Sharma).

using a Jeol, 2010, at 300 kV. Energy dispersive spectroscopy (EDS) analysis was performed using an adjacent Oxford (INCA) system. The quantitative content of zirconium was determined by ICP-MS Agilent 75003 (G3272A). Scanning electron microscope (SEM) images were taken by Gemini Ultra55 (Zeiss). Magnetization curve was obtained by vibrating sample magnetometer (VSM) (EV-9, Microsense). FTIR spectra were recorded on Perkin Elmer Spectrum 2000. The derived products were analyzed using Agilent gas chromatography (6850GC) HP-5MS column (30 m × 0.25 mm × 0.25 μm), 5 mol% phenylmethylpolysiloxane, flow gas He.

2.2. Preparation of catalyst and its applications

2.2.1. Synthesis of amine-functionalized silica coated magnetic nanocomposites

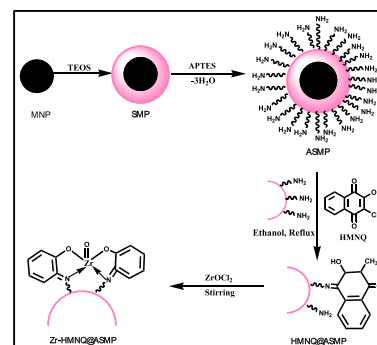
For the synthesis of the magnetic nanoparticles (MNPs) co-precipitation method was used [17]. Coating of these MNPs by silica was performed via sol-gel approach [18]. Silica encapsulated magnetic nanoparticles (SMPs) were functionalized according to the reported procedure [19] using 3-aminopropyltriethoxysilane to afford aminopropylated SMPs (ASMPs).

2.2.2. Synthesis of Zr(IV)-HMNQ complex grafted silica coated magnetic nanocatalyst

3-Hydroxy-2-methyl-1,4-naphthoquinone (HMNQ) was prepared according to the reported procedure [20]. HMNQ (2 mmol) and ASMPs (2 g) were then stirred in absolute ethanol and refluxed for 3 h. The grafted ASMPs (2 g) were stirred with solution of 4 mmol of ZrOCl₂ in acetone for 4 h. The resulted Zr(IV)-HMNQ@ASMPs were separated magnetically, washed with water and dried under vacuum (Scheme 1).

2.2.3. Experimental procedure for transformations

The obtained nanocatalyst was investigated for a number of important organic transformations such as Friedel-Crafts (Table 1), Knoevenagel condensation (Table 2) and Pechmann condensation (Table 3) reactions. Aliquots for reaction monitoring for each of the reaction were removed at regular time intervals and analyzed by GC. After completion of reaction, the catalyst was separated using external magnet (see ESI-S1). Rest of the solution was taken out with pipette and extracted with ethyl acetate, washed with brine solution, dried and



Scheme 1. Sequence of events in the preparation of Zr(IV)-HMNQ@ASMPs.

concentrated to give products. The structure elucidations of the products were confirmed by GC-MS.

3. Results and discussion

3.1. Shape and morphology of the nanoparticles

The size and morphology of the prepared catalyst were characterized by TEM (Fig. 1). MNPs prepared by the chemical co-precipitation are quasi spherical with an average of 7–10 nm as shown in Fig. 1(a). From HR-TEM as shown in Fig. 1(b), the average interfringe distance of MNPs was measured to be ~0.3 nm which, corresponds to (2 2 0) plane of inverse spinel structured Fe₃O₄. The nanoparticles depicted in Fig. 1(c) after silica encapsulation step have a discrete core/shell structure, and their uniform magnetic core is surrounded by a 2–3 nm thick silica shell. Fig. 1(d) reveals the grafting of organic polymer (APTES) onto the surface of silica coated nanoparticles.

The SEM images of nanoparticles before (a) and after (b) encapsulation are shown in Fig. 2. The smooth surface of the magnetic core particles was roughened due to deposition of silica coating to magnetic nanoparticles, which formed uniform and continuous shell around them. Separate silica aggregates are not observed indicating that precipitation of primary silica nanoparticles was performed only on the surface of the functionalized core particles.

Table 1
Friedel-Craft reaction of aldehydes with indoles.

Entry	R ₁	R ₂	Conv. ^a (%)	Select. ^b (%)	TON(TOF) ^c
1.	H	H	99 *99, 98, 98, 97, 96 ^d	100	495(990)
2.	H	4-OCH ₃	96	99	480(960)
3.	H	4-CH ₃	99	96	495(990)
4.	H	4-Cl	94	94	470(940)
5.	2-Me	H	96	99	480(960)
6.	2-Me	4-OCH ₃	95	95	475(950)
7.	2-Me	4-CH ₃	97	99	485(970)
8.	2-Me	4-Cl	95	97	475(950)

Reaction conditions: catalyst (20 mg), aldehyde (1 mmol), indoles (2 mmol) at R.T., time 30 min.

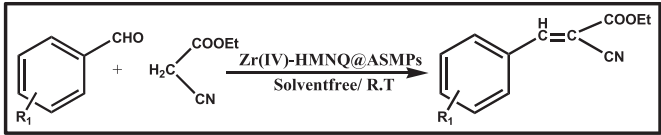
^a Conversion = [(initial moles of substrate – final moles of substrate)/initial moles of substrate] × 100.

^b Selectivity(product) = [desired product%/(total GC peak area% for all the products%)] × 100.

^c TON = number of moles of product per mole of catalyst/TOF = TON per hour.

^d Recycling experiment.

Table 2
Knoevenagel-condensation of aldehydes with ethylcyanoacetate.



Entry	R1	Conv. ^a (%)	Select. ^b (%)	TON(TOF) ^c
1.	H	99 *99, 98, 98, 97, 97 ^d	100	495(1500)
2.	3-NO ₂	95	99	475(1439)
3.	4-OH	97	96	485(1469)
4.	4-OCH ₃	93	99	465(1409)
5.	4-Cl	96	97	480(1454)
6.	4-CH ₃	97	96	485(1469)
7.	Cinnamaldehyde	99	100	495(1500)

Reaction conditions: catalyst (20 mg), aldehyde (1 mmol), ethylcyanoacetate (2 mmol) at R.T., time 20 min.

^a Conversion = [(initial moles of substrate – final moles of substrate)/initial moles of substrate] × 100.

^b Selectivity(product) = [desired product%/(total GC peak area% for all the products%)] × 100.

^c TON = number of moles of product per mole of catalyst/TOF = TON per hour.

^d Recycling experiment.

3.2. Phase and structural characterization of the nanoparticles

X-ray diffraction measurement was performed to investigate the influence of modifications on the structure of the magnetic core surface. XRD patterns of the native MNPs revealed that the positions and the relative intensities of the diffraction peaks matched well with the standard XRD data of JCPDS card number (19-0629) for Fe₃O₄ crystal with a cubic spinel structure (see ESI-S2). The XRD pattern for SMPs showed a weak broad band at $2\theta = 20^\circ$ – 24° which is due to the amorphous silane shell formed around the magnetic core. The broadening of XRD peaks in SMPs is attributed to the decrease in crystalline size of the nanoparticles [21]. Also, there is no any other appreciable shift in the peak positions, which indicates the structural stability of magnetite nanoparticles.

The presence of well resolved peak of zirconium is observed in the EDX spectrum (see ESI-S3) of the Zr(IV)-HMNQ@ASMPs, which confirms the immobilization of zirconium on the HMNQ grafted ASMPs. The zirconium content in catalyst was found to be 0.14 mmol/g using ICP-MS.

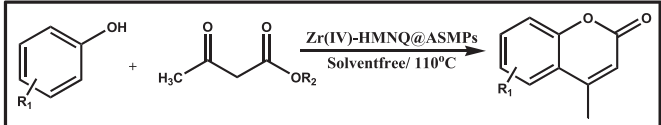
The FT-IR spectroscopy is employed to monitor the immobilization process by comparing the precursor and modified surfaces (see ESI-S4). The spectra of the MNPs showed characteristic of the magnetite

support matrices at 588 cm^{-1} which is assigned to Fe–O stretching vibration [22]. After silica coating of MNPs (SMPs), significant reduction of the intensity of the Fe–O vibration bands is observed, while a broad band appears at 1090 cm^{-1} is assigned to the Si–O stretching vibrations. On functionalization, no major changes are observed, however an extra band at 2926 cm^{-1} appears for $-\text{CH}_2$ stretching of the silylating agent [23]. In case of catalyst, the IR band related to the anchored complex is observed at 1649 cm^{-1} due to C=N stretching vibration. On metallation, C=N frequency decreased to lower wave number (1637 cm^{-1}) indicative for formation of metal–ligand bond.

3.3. Magnetic properties

The magnetization curves of coated, uncoated and zirconium(IV) complex grafted nanocatalyst showed no hysteresis opening with complete reversibility at room temperature. The coercivity and remanence were not observed in any of the curves which confirmed the superparamagnetism of nanoparticles. Fig. S5 (see ESI) showed the decrease in saturation magnetism from 53.45 emu/g of MNPs to 15.06 emu/g of Zr(IV)-HMNQ@ASMPs. The deviation between

Table 3
Pechmann-condensation of phenols with β -keto ester.



Entry	R ₁	R ₂	Conv. ^a (%)	Select. ^b (%)	TON(TOF) ^c
1.	3-OH; 5-OH	OEt	99 *99, 98, 97, 97, 96 ^d	100	495(2981)
2.	2-OH; 3-OH	OEt	98	99	490(2951)
3.	3-OH	OEt	99	96	495(2981)
4.	3-Me	OEt	96	97	480(2891)
5.	3-NH ₂	OEt	98	95	490(2951)
6.	3-OCH ₃	OEt	97	99	485(2921)

Reaction conditions: catalyst (20 mg), phenol (1 mmol), β -keto ester (1 mmol) at 110°C , time 10 min.

^a Conversion = [(initial moles of substrate – final moles of substrate)/initial moles of substrate] × 100.

^b Selectivity(product) = [desired product%/(total GC peak area% for all the products%)] × 100.

^c TON = number of moles of product per mole of catalyst/TOF = TON per hour.

^d Recycling experiment.

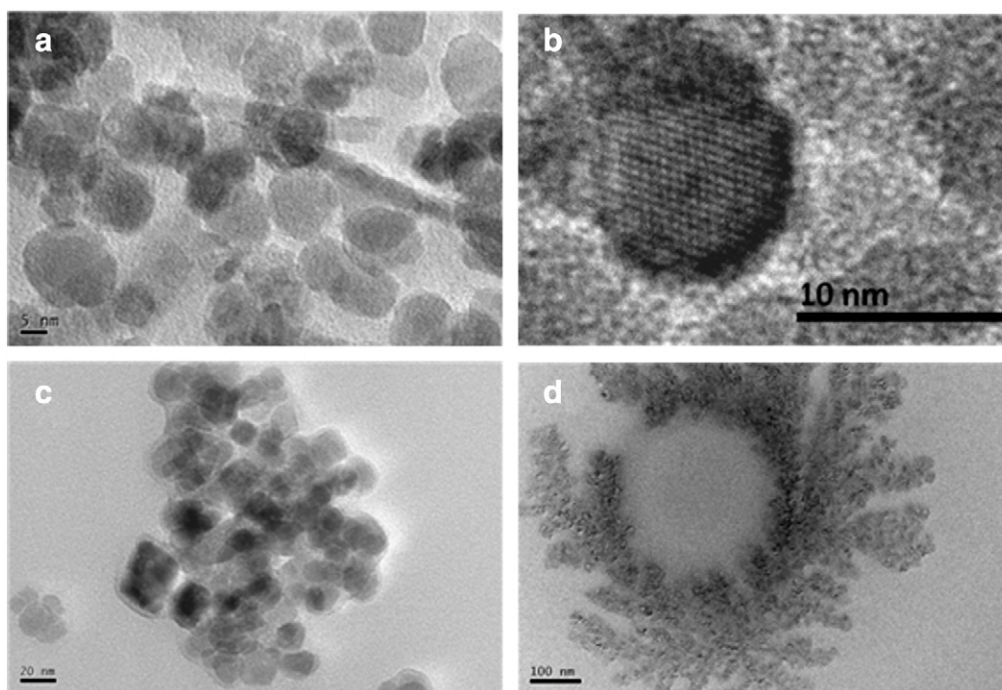


Fig. 1. TEM micrographs of (a) MNPs (b) HR-TEM image (c) SMPs and (d) ASMPs.

them is attributed to the increased mass of diamagnetic silica over MNPs and grafting of metal–ligand complex over ASMPs [24].

3.4. Catalytic studies

To investigate the catalytic activity of organic–inorganic hybrid material different reactions were studied. The reactions did not proceed in the absence of catalyst or only with ASMPs as catalyst. Whereas, Zr(IV)-HMNQ@ASMPs served as an efficient catalyst for the reactions with highest conversion and selectivity. This indicated that the reaction is catalyzed by Zr(IV). The use of metal salt ($ZrOCl_2$) as homogeneous catalyst showed quite poor activity pointing out the importance of the HMNQ ring (Table S2). In this case, HMNQ with strong σ donating ability of nitrogen and oxygen donor acted as a co-catalyst and also anchored the Zr(IV) in a better way. In addition, this homogeneous catalyst decomposed after the reaction and could not be reused. To obtain best catalytic activity, reaction conditions were optimized using different solvents and solvent-free conditions (Fig. S6). Interestingly, under solvent free condition, maximum conversion was obtained in all three cases. Hence, all the reactions were carried in solvent free conditions. As far as effect of temperature is concern, only Pechmann

condensation of coumarins showed a drastic change in the reaction time period and product yield with increasing temperature (Fig. S7). Whereas, the other two reactions were not showed significant changes, hence these reactions were optimized at room temperature. As can be seen from Tables 1, 2 and 3, the catalytic system worked exceedingly well in all the three cases with a wide range of substrates.

3.5. Catalyst stability and reusability

To analyze the heterogeneity of catalyst, the reactions were carried out using Zr(IV)-HMNQ@ASMPs as catalyst under the conditions indicated in Tables 1, 2, and 3 and the solid Zr(IV) nanocatalyst was removed magnetically at about half the specified reaction time period. Then, the filtrate was allowed to react under the same conditions. After separation of catalyst, no further conversion of the reactant was found. The ICP-MS analysis of the post reaction mixture showed no detectable (<0.01 ppm) zirconium, which further signifies the stability and heterogeneity of prepared nanocatalyst.

For testing the recoverability, the separated catalyst has been reused for five consecutive reaction cycles in all the three cases. The conversion of the reactant after five cycles was almost constant and

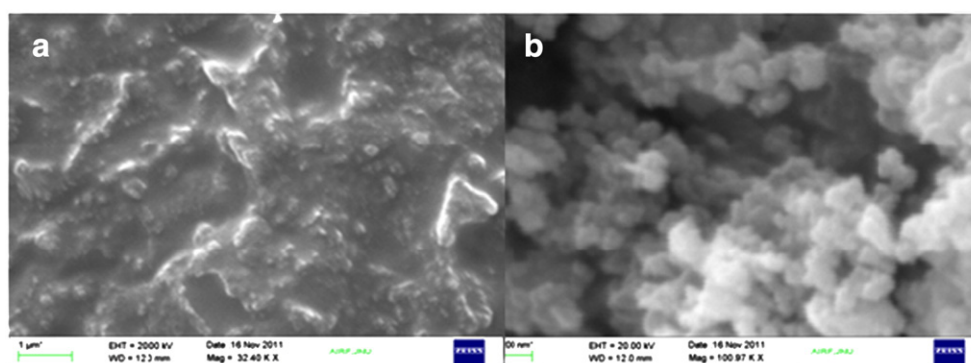


Fig. 2. SEM images of (a) MNPs and (b) SMPs.

no loss of catalytic activity and selectivity as compared with the fresh catalyst was observed. Comparison of the TEM image of fresh and re-covered catalysts depicts that the structural and morphological properties of the anchored complex remain unaltered (Fig. S8).

4. Conclusions

In conclusion, we have developed an environmentally benign protocol for the synthesis of industrially significant product under fast, simple, effective and environmentally benign conditions. Mild reaction conditions, high activity and selectivity, economic viability, easy preparation and reusability of the catalyst make the present protocol a greener alternative.

Acknowledgments

Due thanks are given to USIC-CLF, DU, Delhi, India for HR-XRD, HR-TEM and VSM analyses.

Appendix A. Supplementary data

Supplementary data to this article can be found online at <http://dx.doi.org/10.1016/j.catcom.2013.02.016>.

References

- [1] R. Schlogl, S.B.A. Hamid, *Angewandte Chemie International Edition* 43 (2004) 1628–1637.
- [2] Y. Zhu, L.P. Stubbs, F. Ho, R. Liu, C.P. Ship, J.A. Maguire, N.S. Hosmane, *ChemCatChem* 2 (2010) 365–374.
- [3] V. Polshettiwar, R. Luque, A. Fihri, H. Zhu, M. Bouhrara, J.M. Basset, *Chemical Reviews* 111 (2011) 3036–3075.
- [4] T. Zeng, L. Yang, R. Hudson, G. Song, A.R. Moores, C.J. Li, *Organic Letters* 13 (2011) 442–445.
- [5] E. Rafiee, S. Eavania, *Green Chemistry* 13 (2011) 2116–2122.
- [6] G.D. Yadav, N.P. Ajgaonka, A. Varma, *Journal of Catalysis* 292 (2012) 99–110.
- [7] A. Sinhamahapatra, N. Sutradhar, S. Pahari, H.C. Bajaj, A.B. Panda, *Applied Catalysis A: General* 394 (2011) 93–100.
- [8] R.K. Sharma, C. Sharma, *Catalysis Communications* 12 (2011) 327–331.
- [9] R.K. Sharma, S. Gulati, A. Panday, *Applied Catalysis B: Environmental* 125 (2012) 247–258.
- [10] R.K. Sharma, A. Panday, S. Gulati, *Applied Catalysis A: General* 431 (2012) 33–41.
- [11] R.K. Sharma, D. Rawat, G. Gaba, *Catalysis Communications* 19 (2012) 31–36.
- [12] R.K. Sharma, S. Gulati, *Journal of Molecular Catalysis A: General* 363 (2012) 291–303.
- [13] R.K. Sharma, Y. Monga, *Applied Catalysis A: General*, DOI-<http://dx.doi.org/10.1016/j.apcata.2012.12.046>.
- [14] C. Karami, H. Ahmadian, M. Nouri, F. Jamshidi, H. Mohammadi, K. Ghodrati, A. Farrokhi, Z. Hamidi, *Catalysis Communications* 27 (2012) 92–96.
- [15] K.M. Parida, S. Mallick, P.C. Sahoo, S.K. Rana, *Applied Catalysis B: Environmental* 381 (2010) 226–232.
- [16] B. Karami, M. Kiani, *Catalysis Communications* 14 (2011) 62–67.
- [17] V. Polshettiwar, R.S. Varma, *Organic & Biomolecular Chemistry* 7 (2009) 37–40.
- [18] Z. Zhang, F. Zhang, Q. Zhu, W. Zhao, B. Ma, Y. Ding, *Journal of Colloid and Interface Science* 360 (2011) 189–194.
- [19] O. Kuhl, *Chemical Society Reviews* 36 (2007) 592–607.
- [20] B.S. Garg, J.S. Bist, R.K. Sharma, N. Bhojak, *Talanta* 43 (1996) 2093–2099.
- [21] R.A. Reziq, D. Wang, M.L. Post, H. Alper, *Journal of the American Chemical Society* 128 (2006) 5279–5280.
- [22] M. Yamaura, R.L. Camilo, L.C. Sampaio, M.A. Macedo, M. Nakamura, H.E. Toma, *Journal of Magnetism and Magnetic Materials* 279 (2004) 210–217.
- [23] M.M. Farahani, N. Tayyebi, *Journal of Molecular Catalysis A: Chemical* 348 (2011) 83–87.
- [24] M.R. Liane, P.S. Fernanda, L.R.V. Lucas, K.K. Pedro, L.D. Evandro, I. Rosangela, L. Richard, M. Giovanna, *Green Chemistry* 9 (2007) 379–385.